Def Sci J, Vol 32, No 3, July 1982, pp 175-187

Exterior Problem of a Finite Cylindrical Cavity in Elasto-Dynamics

JAGDISH CHANDRA, RAM KUMAR & K. VISWANATHAN
Defence Science Centre, Metcalfe House, Delhi-110 054

Received 6 December 1980; revised 25 August 1981

Abstract. The elasto-dynamic problem of a finite cylindrical cavity in an infinite elastic solid has been studied. In order to satisfy the radiation conditions at infinity, the solution has been assumed in terms of Spherical Hankel functions and in order to satisfy the conditions at the boundary of the cavity, the method of least square approximation has been used for the minimisation of the errors on the boundary. The radiation patterns of displacements are given for two sets of frequencies and aspect ratios.

1. Introduction

It is well known that the solution of certain class of problems in elasticity and acoustics are not satisfactorily carried out by the method of separation of variables. An important problem of this class is one which involves a finite cylindrical geometry. Although the interior problem has recently been analysed by a powerful method of superposition of the modes of the dominant part of boundary[1,2,3,4], the corresponding exterior problem is not yet fully solved. The difficulty is in finding appropriate cylindrical functions which would be required to satisfy the three dimensional radiation condition at infinity.

Accordingly, alternative methods have been attempted for the exterior problem. Williams[5] *et al.* investigated the acoustic radiation from a finite cylinder using a solution in the form of Spherical Hankel functions. The boundary of the cylinder was treated as one continuous curve in the axial plane and a least-square approximation was applied for the minimization of the errors on the boundary. For selected wave numbers ($ka = 1$, 2 and 5; height $= 4a$, where a is the radius of the cylinder) they obtained far-field radiation patterns and compared with the results due to a line source as well as due to loading over an infinite cylindrical cavity.

In this paper, we employ the above technique to the more difficult problem of a finite cylindrical cavity in an infinite elastic medium which arises in the contexts of explosive working, geophysical prospecting and under-ground explosions. The solution obtained here takes into account the special nature of the edges of the cydrical cavity. A proof of convergence validating the spherical function expansion of the

solution pertaining to cylindrical geometries is given separately as the appendix to the paper.

2. Formulation of the Problem

In the cylindrical system r, ϕ, z, let the elastic solid occupy the exterior of the cylindrical cavity as shown in Fig. 1.

$$r = a, \ |z| < b; \ |z| = b, r < a \text{ with } 0 \leqslant \phi \leqslant 2\pi.$$

The equations of motion are given by

$$(\lambda + \mu) \text{ grad div } \vec{U} + \mu \nabla^2 \vec{U} = \rho \frac{\partial^2 \vec{U}}{\partial t^2} \tag{1}$$

where λ, μ are Lame's constants, ρ is the density and $\vec{U}$ is the displacement vector. No body-forces are assumed.

For axi-symmetric, time-harmonic loading on the boundary, the solution of (1) can be taken as follows

$$\begin{aligned} u_r &= \frac{\partial \Phi}{\partial r} + \frac{\partial^2 \psi}{\partial r \partial z} \\ u_\phi &= 0 \\ u_z &= \frac{\partial \Phi}{\partial z} - \frac{1}{r} \frac{\partial}{\partial r}\left(r \frac{\partial \psi}{\partial r}\right) \end{aligned} \tag{2}$$

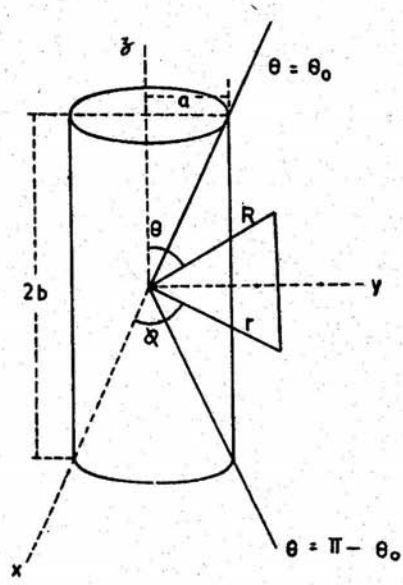

Figure 1. Coordinates and notation for finite-cylinder.

where Φ and ψ statisfy the Helmholtz equations

$$(\nabla^2 + k_\alpha^2)\,\Phi = 0$$

$$(\nabla^2 + k_\beta^2)\,\psi = 0 \tag{3}$$

and $\quad k_\alpha = \omega/\alpha,\ k_\beta = \omega/\beta,\ \alpha^2 = (\lambda + 2\mu)/\rho,\ \beta^2 = \mu/\rho$

where ω is the circular frequency in the harmonic factor $e^{i\omega t}$. The conditions for the normal and shear stresses on the cavity are taken to be

$$\sigma_n = \mu F(\theta)\, e^{i\omega t}$$

$$\tau_{ns} = \mu G(\theta)\, e^{i\omega t},\ (0 \leqslant \theta \leqslant \pi) \tag{4}$$

where R, θ, ϕ denote the spherical co-ordinates. In the above equations, it is assumed that the surface of the cylindrical cavity is given by the piece-wise continuous curve (in the axial plane)

$$R = b \sec\theta \left(0 \leqslant \theta < \tan^{-1}\frac{a}{b} \text{ and } \pi - \tan^{-1}\frac{a}{b} < \theta \leqslant \pi\right)$$

$$R = a \operatorname{cosec}\theta \left(\tan^{-1}\frac{a}{b} \leqslant \theta \leqslant \pi - \tan^{-1}\frac{a}{b}\right) \tag{5}$$

In addition to Eqn. (4), the radiation condition at infinity must also be satisfied. Accordingly, we assume that the solution of Eqn. (3) in terms of outgoing spherical wave functions as follows

$$\Phi = \sum_{n=0,1,2} a_n h_n^{(2)}(k_\alpha R)\, P_n(\cos\theta)$$

$$\psi = \sum_{n=0,1,2} b_n h_n^{(2)}(k_\beta R)\, P_n(\cos\theta) \tag{6}$$

where $h_n^{(2)}$ are the spherical Hankel functions of second kind and $P_n(\cos\theta)$ is the Legendre polynomial of order n. a_n and b_n are arbitrary co-efficients, which are to be determined. The convergence of such solutions for cylindrical boundaries is discussed through an example in the Appendix.

3. Method of Solution by the Least Square Approximation

The normal and shear stresses due to Eqn. (6) on the cavity are given by

$$\sigma_n = \mu N(\theta) = \sum \left\{ a_n A_n^{11}(\theta) + b_n A_n^{12}(\theta) \right\}$$

$$\tau_{ns} = \mu T(\theta) = \sum \left\{ a_n A_n^{21}(\theta) + b_n A_n^{22}(\theta) \right\} \tag{7}$$

where $A_n^{ij}(\theta)$ are defined as

$$\begin{bmatrix} A_n^{11}(\theta) \\ A_n^{21}(\theta) \end{bmatrix} = \begin{bmatrix} -\lambda k_\alpha^2 + 2\mu L_1 \\ 2\mu \dfrac{\partial^2}{\partial r \partial z} \end{bmatrix} h_n^{(2)}(k_\alpha R) P_n(\cos\theta)$$

and

$$\begin{bmatrix} A_n^{12}(\theta) \\ A_n^{22}(\theta) \end{bmatrix} = \begin{bmatrix} L_2 \\ \left(2\dfrac{\partial^3}{\partial r \partial z^2} + k_\beta^2 \dfrac{\partial}{\partial r}\right) \end{bmatrix} h_n^{(2)}(k_\beta R) P_n(\cos\theta)$$

where

$$L_1 = \begin{cases} \dfrac{\partial^2}{\partial r^2} \text{ for } \theta_0 < \theta < \pi - \theta_0 \\ \dfrac{\partial^2}{\partial z^2} \text{ for } 0 < \theta < \theta_0 \text{ and } \pi - \theta_0 < \theta < \pi \end{cases}$$

and

$$L_2 = \begin{cases} 2\mu \dfrac{\partial^3}{\partial r^2 \partial z} \text{ for } \theta_0 < \theta < \pi - \theta_0 \\ -2\mu\left(\dfrac{\partial^3}{\partial r^2 \partial z} + \dfrac{1}{r}\dfrac{\partial^2}{\partial r \partial z}\right) \text{ for } 0 < \theta < \theta_0 \text{ and } \pi - \theta_0 < \theta < \pi \end{cases}$$

Since the boundary is treated as one curve, the edges of the cylinder have to be specially represented. We have, accordingly, assumed a small circular arc to replace the edge concerned so that the values of the normal and shear stresses can be compounded by the formulae[6],

$$\begin{aligned} \sigma_n &= \tfrac{1}{2}(\sigma_r + \sigma_z + 2\tau_{rz}) \\ \tau_{ns} &= \tfrac{1}{2}(\sigma_r - \sigma_z) \end{aligned} \tag{8}$$

From the geometrical point of view this representation of the edges is good enough. But, to achieve more accurate results, the prescribed boundary conditions should also influence the form of this representations. With this observation, the boundary conditions in Eqn. (4) are effectively satisfied by requiring that the folowing integral is minimized

$$\begin{aligned} I &= \mu^2 \int_0^\pi \{ |F(\theta) - N(\theta)|^2 + |G(\theta) - T(\theta)|^2 \} dS(\theta) \\ &= I_N + I_T \text{ (say)} \end{aligned} \tag{9}$$

where $dS(\theta) = -2\pi a \operatorname{cosec}^2\theta d\theta$ on the lateral surface of the cavity ($r = a$) and $dS(\theta) = 2\pi b^2 \tan\theta \sec^2\theta d\theta$ on the flat surface ($z = \pm b$). The conditions for the minimization of the above integral are

$$\frac{\partial I}{\partial a_n} = 0 \text{ and } \frac{\partial I}{\partial b_n} = 0 \tag{10}$$

where n takes all the values as in Eqn. (6). Using the expressions for $N(\theta)$ and $T(\theta)$ from Eqn. (7), this gives an infinite system of equations for a_n and b_n. The equations are given by

$$\mu \int_0^{\pi} \sum_m \{F(\theta)\ \bar{A}_m^{11}(\theta) + G(\theta)\,\bar{A}_m^{21}(\theta)\}\, dS(\theta)$$

$$= \int_0^{\pi} \sum_n \sum_m \{a_n A_n^{11}(\theta)\,\bar{A}_m^{11}(\theta) + b_n A_n^{12}(\theta)\,\bar{A}_m^{11}(\theta)\}\, dS(\theta)$$

$$+ \int_0^{\pi} \sum_n \sum_m \{a_n A_n^{21}(\theta)\,\bar{A}_m^{21}(\theta) + b_n A_n^{22}(\theta)\,\bar{A}_m^{21}(\theta)\}\, dS(\theta).$$

$$\mu \int_0^{\pi} \sum_m \{F(\theta)\,\bar{A}_m^{12}(\theta) + G(\theta)\,\bar{A}_m^{22}(\theta)\}\, dS(\theta)$$

$$= \int_0^{\pi} \sum_n \sum_m \{a_n\, A_n^{11}(\theta)\,\bar{A}_m^{12}(\theta) + b_n A_n^{12}(\theta)\,\bar{A}_m^{12}(\theta)\}\, dS(\theta)$$

$$+ \int_0^{\pi} \sum_n \sum_m \{a_n\, A_n^{21}(\theta)\,\bar{A}_m^{22}(\theta) + b_n\, A_n^{22}(\theta)\,\bar{A}_m^{22}(\theta)\}\, dS(\theta) \tag{11}$$

where

$$m = 0, 1, 2, \ldots\ldots$$

$$n = 0, 1, 2, \ldots\ldots$$

and $\bar{A}_m^{ij}$ are the complex conjugates of A_m^{ij}

In order to make the solution feasible, we truncate this system of equations by restricting the range of m, n, (say $m, n \leqslant N$) which gives a finite set of equations for $a_n's$ and $b_n's$. Solving this finite set of equations the stresses and displacements in the medium can be found in terms of the various parameters of the problem. The discussion of our numerical investigations is given in the next section.

4. Numerical Results

Let us choose the loading functions $F(\theta)$, $G(\theta)$ in Eqn. (4) as follows

$$F(\theta) = 1$$

$$G(\theta) = \sin(2\theta) \tag{12}$$

Since the above loading functions have symmetry about the plane $z = 0$ we need to take only given terms in Φ and odd terms in ψ in the trial solution in Eqn. (6). The

computations of the coefficients and the stresses were carried out in the following two stages (taking $\lambda = \mu$)

Stage 1

Here we fixed the value of $k_\beta a$, taking $k_\beta a = 2.0$. The coefficients were then obtained from Eqn. (11) for $m, n \leqslant 9$ and for several values of the aspect ratio (b/a). Our aim, firstly, was to estimate the minimum values of integral of errors I defined in Eqn. (9). To make this estimation more valuable, the two terms in Eqn. (9), which represent the errors due to normal stress and shear stress, respectively, were separately calculated. These results are given in Table 1 for $0.85 \leqslant b/a \leqslant 1.60$.

Table 1. Values of error integrals for $k_\beta a = 2.0$ ($I = I_N + I_T$)

Aspect ratio (b/a)	Integral of sq. of normal stress difference (I_N)	Integral of sq. of shear stress difference (I_T)
0.850	0.134	0.235
0.900	0.215	0.478
0.905	0.145	0.126
0.912*	0.127	0.129
0.913	0.171	0.135
0.914	0.188	0.138
0.920	0.267	0.169
0.950	0.119	0.143
1.000	0.112	0.149
1.100	0.127	0.148
1.200	0.134	0.160
1.300	0.138	0.168
1.400	0.139	0.153
1.600	0.189	0.142

*Indicates optimum value with least error.

It can be seen from table 1 that the errors are minimum for the case when $b/a = 0.912$. We also extended calculations for the values of b/a exceeding 1.60 and the errors were found to increase continuously. It is seen that the above minimum value of b/a could be a characteristic aspect ratio for $k_\beta a = 2.0$. The coefficients a_n and b_n for this case are given in Table 2. These are seen to decrease rapidly.

Table 2. Expansion coefficients for the finite cylinder with $b/a = 0.912$, $k_\beta a = 2.0$.

n	Expansion coefficient (a_n)	n	Expansion coefficient (b_n)
0	$-0.145840 - i\,0.3473911$	1	$-0.1783688 \times 10^{-1} + i\,0.1182775$
2	$-0.1420276 \times 10^{-1} + i\,0.15524202 \times 10^{-1}$	3	$-0.4474719 \times 10^{-1} - i\,0.1372831$
4	$-0.3662128 \times 10^{-2} - i\,0.1155389 \times 10^{-1}$	5	$0.5053810 \times 10^{-3} + i\,0.6201523 \times 10^{-3}$
6	$0.1337902 \times 10^{-4} - i\,0.1692105 \times 10^{-4}$	7	$-0.1918884 \times 10^{-5} + i\,0.2705217 \times 10^{-5}$
8	$-0.1696019 \times 10^{-7} + i\,0.2750128 \times 10^{-7}$	9	$-0.1023868 \times 10^{-9} + i\,0.3165012 \times 10^{-8}$

The amplitudes of the stresses on the cavity reproduced by our solution for the above case ($k_\beta a = 2$, $b/a = 0.912$) are shown in Fig. 2 and compared with the prescribed values. The shear stress generally follows the pattern of the prescribed load very closely with a slight deviation near the edge of the cavity. The normal stress tends to oscillate about the prescribed load. However, the integrated values of the errors (I_N), is not high. For, this is of the order of 0.127 for normal stresses while the shear contribution (I_T) is also of the order of 0.129. (The values 0.127 and 0.129 for the errors I_N & I_T are to be interpreted in the sence of 'variances' with error distributions). In all these curves the regions of flat and lateral surfaces are separated for the sake of clarity.

Stage 2

This is similar to stage 1 excepting that we now fix b/a and vary $k_\beta a$. The results are given in Table 3 and Fig. 3.

Table 3. Values of error integrals for $b/a = 2.0$ ($I = I_N + I_T$)

$k_\beta a$	Integral of sq. of normal stress difference (I_N)	Integral of sq. of shear stress difference (I_T)
1.00	0.127×10^5	0.964×10^4
1.40	0.273×10^3	0.218×10^3
1.60	0.455×10^1	0.326×10^1
2.00	0.458	0.256
2.20	0.375	0.324
2.60	0.222	0.206
3.00	0.221	0.249
3.20	0.227	0.253
3.40	0.230	0.237
3.60	0.243	0.221
3.90	0.242	0.161
4.00	0.242	0.154
4.05	0.242	0.151
4.10	0.245	0.147
4.15*	0.221	0.129
4.30	0.246	0.144
4.50	0.252	0.154
4.80	0.255	0.164

(*Indicates optimum value with least error).

Radiation patterns for the displacements are plotted in Figs. 4 and 5 for the above cases.

5. Conclusion

We have attempted to solve the elasto-dynamic problem of a finite cylindrical cavity with the help of spherical Hankel Functions which automatically satisfy the radiation

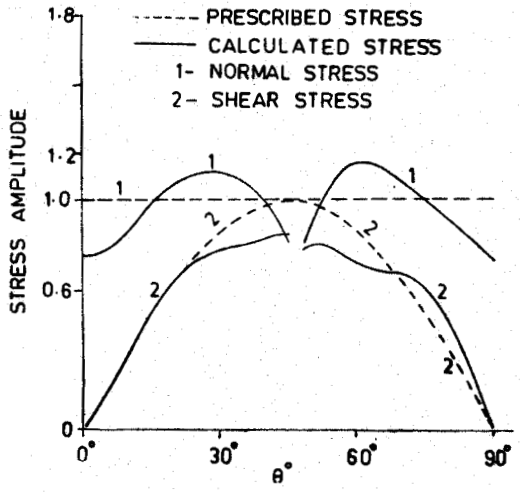

Figure 2. Stress amplitude *vs* θ (in degrees) on the surface of the cylinder (Aspect ratio $b/a = 0.912$, $k_\beta a = 2.0$).

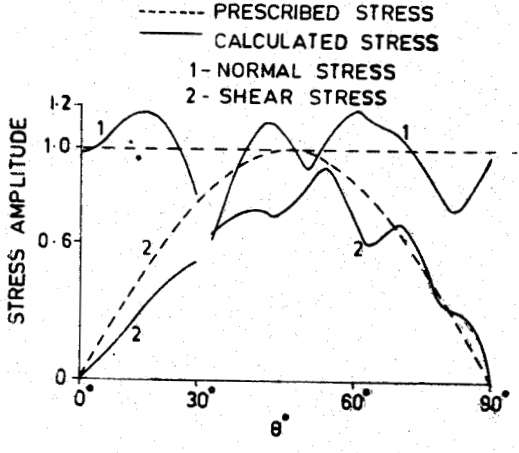

Figure 3. Stress amplitude *vs* θ (in degrees) on the surface of the cylinder (Aspect ratio $b/a = 2.0$ & $k_\beta a = 4.15$).

conditions at infinity. We have also used the least-square approximation for satisfying the boundary conditions. In addition, a simple scheme for rounding off the edges of the boundary has been adopted. Computation suggests that for any given wave numbers (aspect ratios) the solution with least errors can be tracked in the neighbourhood of some corresponding aspect ratios (wave numbers). In order to obtain the solution for any arbitrary pair of values of both these parameters, the techniques may have to be improved in one of the following lines :

(*a*) By including more terms in the trial solution; (*b*) By using spheroidal wave functions in place of spherical wave functions; or (*c*) By using a better scheme, if available, both in place of least square method as well as for treating the edges of the cavity.

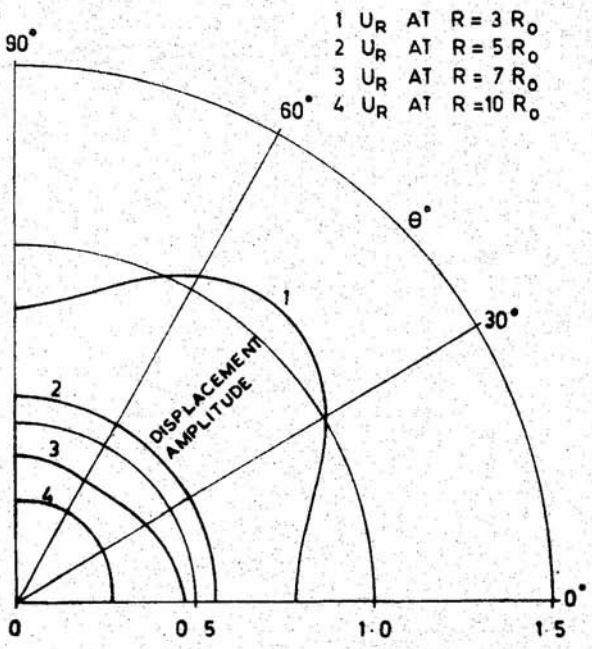

Figure 4(a). Radial displacement amplitude *vs* θ (in degrees) for $k_\beta a = 2.0$ and $b/a = 0.912$; $(R = \sqrt{(r^2 + z^2)}/a, R_0 = \sqrt{(b^2 + a^2)}/a)$.

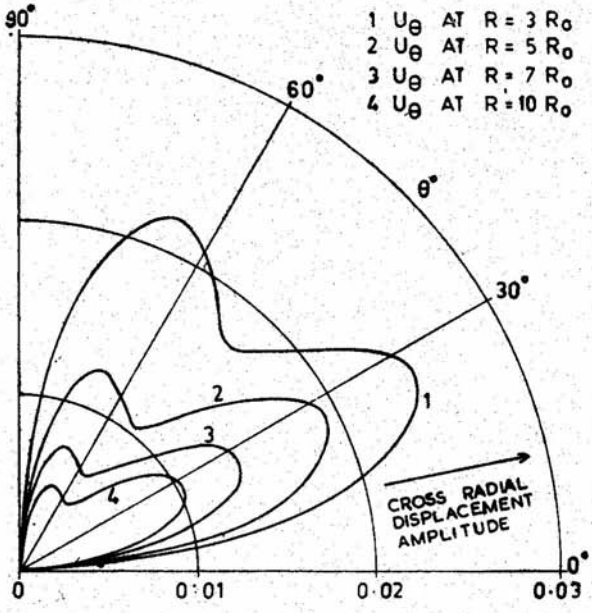

Figure 4(b). Cross radial displacement amplitude *vs* θ (in degrees) for $k_\beta a = 2.0$ and $b/a = 0.912$; $(R = \sqrt{(r^2 + z^2)}/a, R_0 = \sqrt{(b^2 + a^2)}/a)$.

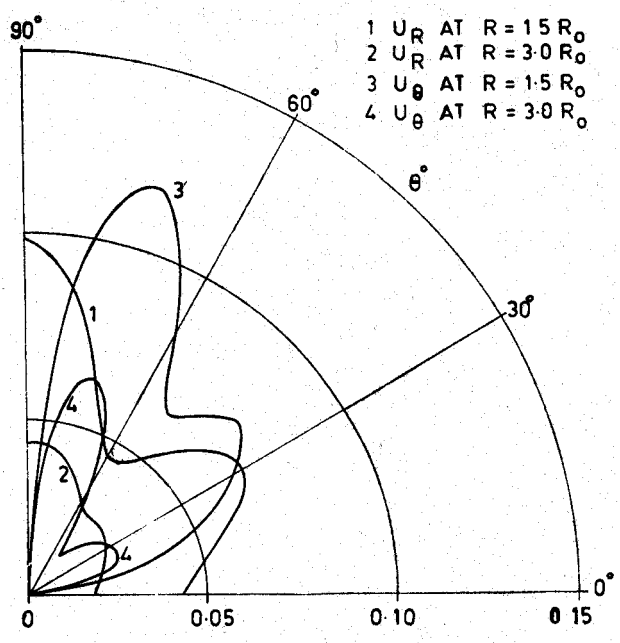

Figure 5. Displacement amplitude *vs* θ (in degrees) for $k_\beta a = 4.15$ and $b/a = 2.0$; $(R = \sqrt{r^2 + z^2})/a$, $R_0 = \sqrt{(b^2 + a^2)}/a$).

References

1. Ram Kumar, *J. Accoust, Soc. Am.*, **38** (1965), 851–854.
2. Ram Kumar, *Acustica.*, **34** (1976), 281.
3. Jagdish Chandra & Ram Kumar, *Acustica*, **38** (1977), 23.
4. Jagdish Chandra & Ram Kumar, *Acustica*, **38** (1977), 257.
5. Williams, W., Parks, N. G., Moran, D. A. & Sherman, C. H., *J. Acoust. Soc. Am.*, **36** (1965), 2316–2322.
6. Alterman, Z. & Lowenthal. D., *Geophys, J. R. Astr. Soc.*, **20** (1970), 101–126.

Appendix

Proof of convergence of the technique

We establish the convergence of the solutions of the type given in Eqn. (6) with the help of a simple example. The essential point will be to prove the convergence right upto the surface of the cylindrical cavity.

Consider the series

$$\chi = \Sigma \chi_n = \sum_{n=0}^{\infty} a_n h_n(kR) P_n (\cos \theta) \tag{1}$$

with the boundary condition, say, of the Dirichlet type

$$\chi \equiv \chi(P_s) = \alpha_s \tag{2}$$

where P_s is a point on the cylindrical cavity. Let us now solve this problem by taking the first $(n + 1)$ term of the series (1) and satisfying the condition (2) at $(n + 1)$ selected points $P_0, P_1 \ldots, P_n$ on the cavity which include the nearest point P_n and the fartherst point P_o of the cavity from its centre. This gives rise to the following equations for determining $a_0, a_1, \ldots\ldots a_n$

$$\sum_{i=0}^{n} a_i H_i(P_j) = \alpha_j (j = 0, 1, 2, \ldots n) \tag{3}$$

where

$$H_m(P_j) = \{h_m(kR)\, P_m(\cos\theta)\}_{P=P_j} \tag{4}$$

The solution of Eqn. (3) is

$$a_p = \Delta_p/\Delta \tag{5}$$

where

$$\Delta = \{H_i(P_j)\} \tag{6}$$

while Δ_p can be obtained from the Cramer's rule in the form

$$\Delta_p = (N_{ij}) \tag{7}$$

where $N_{ij} = H_i(P_j)$, $i \neq p$ and $N_{pj} = \alpha_j$ (for each given p). We observe that Δ can be expanded with its constituent terms of the type.

$$\Sigma\,(\pm)\, H_o(P_p)\, H_1(P_q) \ldots H_n(P_t) \tag{8}$$

where $p, q, \ldots t$ take the values from 0 to n and $p \neq q \neq \ldots t$. To establish the most dominant term here, we note that

$$\begin{aligned} &| P_n(\cos\theta) | < 1, \\ &h_0(z) \sim i/z, \\ &h_n(z) \sim i\,\frac{1.3.5 \ldots (2n-1)}{z^{n+1}},\ n \geqslant 1 \\ &\quad (|z| < < n) \end{aligned} \tag{9}$$

Using Eqn. (9) in Eqn. (4), we get

$$\begin{aligned} &| H_0(P_j) | \sim 1/R_j \\ &| H_n(P_j) | \sim \frac{1.3.5 \ldots (2n-1)}{k^{n+1} R_j^{n+1}},\ n \geqslant 1,\ | kR_j | < < n. \end{aligned} \tag{10}$$

where R_j is the distance of the point P_j of the cylindrical cavity from its centre. If the points $P_0, P_1, P_2, \ldots, P_n$ are so arranged that the distances $R_0, R_1, R_2 \ldots R_n$ are in decreasing order, with $R_0 = (a^2 + b^2)^{1/2}$ and $R_n = \min(a, b)$ then the most dominant term of Δ in Eqn. (8) works out to be

$$\Delta \sim \left(\frac{1}{kR_0}\right)\left(\frac{1}{k^2R_1^2}\right)\left(\frac{1.3}{k^3R_2^3}\right) \ldots \left(\frac{1.3.5 \ldots (2n-1)}{k^{n+1}R_n^{n+1}}\right) \tag{11}$$

Similarly, in the case of Δ_p, we get

$$\Delta_p \sim \left(\frac{1}{kR_0}\right)\left(\frac{1}{k^2R_1^2}\right)\cdots\left(\frac{1.3\ldots\{2(p-2)-1\}}{k^{p-1}R_{p-2}^{p-1}}\right)$$
$$\left(\frac{1.3\ldots\{2(p-1)-1\}}{k^pR_{p-1}^p}\right)\left(\frac{1.3\ldots\{2(p+1)-1\}}{k^{p+2}R_{p+1}^{p+2}}\right)$$
$$\cdots\left(\frac{1.3\ldots(2n-1)}{k^{n+1}R_n^{n+1}}\right) \tag{12}$$

In obtaining Eqns. (11) and (12), we have used the asymptotic approximations in Eqns. (9) and (10) assuming $|z| << n$ for all n. If $|z| << n$ only for $n \geqslant N$ where N is a fixed integer, then the only change in our subsequent argument will be such that we will obtain a modified external factor in place of $(x_0 . x_1 . x_2 \ldots x_n)$ in Eqns. (17) and (18). Using Eqns. (11) and (12) in Eqn. (5), one gets

$$\frac{a_p \sim (kR_p)^{p+1}}{1.3.5\ldots(2p-1)} \tag{13}$$

Thus from Eqns. (1), (9) and (13), we get

$$|\chi_p| \sim \left\{\frac{1.3.5\ldots(2p-1)}{(kR)^{p+1}}\right\}(k^{p+1})\left\{\frac{R_p^{p+1}}{1.3.5\ldots(2p-1)}\right\}$$
$$\sim \frac{R_p^{p+1}}{R^{p+1}}$$
$$= x_p^{p+1} \text{ (say)} \tag{14}$$

where $x_p = (R_p/R)$ and $x_0 > x_1 > x_2 \ldots > x_n$.

Let P be any point at a distance R from the centre of the cavity. P may lie on the cavity or anywhere outside it and not necessarily outside the sphere of radius $(a^2 + b^2)^{1/2}$. For any given value of R, we can find a suitable positive integer m such that $R_p < R$ (i.e. $x_p < 1$) for all $p \geqslant m$ where R_p denotes any point in the set $(R_0R_1 \ldots R_n)$. Note that when $R > R_0$, $m = 0$ while when $R \leqslant R_0$, m will be a definite integer which depends on the value of R.

Now write

$$\sum_{p=1}^{n\geqslant 1} |\chi_p| = \sum_{p=1}^{m-1} |\chi_p| + \sum_{p=m}^{n\geqslant 1} |\chi_p| \tag{15}$$

where

$$\sum_{p=m}^{n\geqslant 1} |\chi_p| \sim \sum_{p=m}^{n\geqslant 1} x_p^{p+1} \text{ from Eqns. (14).} \tag{16}$$

Since $x_0 > x_1 > x_2 \ldots > x_n$ and $x_p < 1$ for $p \geqslant m$, we have

$$\sum_{p=m}^{n \geqslant 1} | \chi_p | < x_m^{m+1} (1 + x_m + x_m^2 + \ldots + x_m^{n-m} \tag{17}$$

Thus as $n \to \infty$

$$\sum_{p=m}^{\infty} | \chi_p | < \frac{x_m^{m+1}}{(1 - x_m)}, \text{ Since } x_m < 1. \tag{18}$$

From Eqns. (15) and (18), it follows that the series (1) is absolutely convergent at all points P everywhere on and outside the cylindrical cavity.

This completes the proof of validity of our technique as the extension of the above proof to the case of least-square approximation is only formal.